Geomechanics and Engineering, *Vol. 14, No. 4 (2018) 345-354*
DOI: https://doi.org/10.12989/gae.2018.14.4.345

A laboratory and numerical study on the effect of geogrid-box method on bearing capacity of rock-soil slopes

Gholam Moradi[1a], Arvin Abdolmaleki[1b], Parham Soltani[*2] and Masoud Ahmadvand[3c]

[1]*Faculty of Civil Engineering, University of Tabriz, Tabriz, Iran*
[2]*Department of Textile Engineering, Isfahan University of Technology, Isfahan 84156-83111, Iran*
[3]*Dimond Consulting Engineers Company, Tehran, Iran*

(Received February 9, 2017, Revised July 18, 2017, Accepted August 9, 2017)

Abstract. Currently, layered geogrid method (LGM) is the commonly practiced technique for reinforcement of slopes. In this paper the geogrid-box method (GBM) is introduced as a new approach for reinforcement of rock-soil slopes. To achieve the objectives of this study, a laboratory setup was designed and the slopes without reinforcements and reinforced with LGM and GBM were tested under the loading of a circular footing. The effect of vertical spacing between geogrid layers and box thickness on normalized bearing capacity and failure mechanism of slopes was investigated. A series of 3D finite element analysis were also performed using ABAQUS software to supplement the results of the model tests.
The results indicated that the load-settlement behavior and the ultimate bearing capacity of footing can be significantly improved by the inclusion of reinforcing geogrid in the soil. It was found that for the slopes reinforced with GBM, the displacement contours are widely distributed in the rock-soil mass underneath the footing in greater width and depth than that in the reinforced slope with LGM, which in turn results in higher bearing capacity. It was also established that by reducing the thickness of geogrid-boxes, the distribution and depth of displacement contours increases and a longer failure surface is developed, which suggests the enhanced bearing capacity of the slope. Based on the studied designs, the ultimate bearing capacity of the GBM-reinforced slope was found to be 11.16% higher than that of the slope reinforced with LGM. The results also indicated that, reinforcement of rock-soil slopes using GBM causes an improvement in the ultimate bearing capacity as high as 24.8 times more than that of the unreinforced slope.

Keywords: stabilization; rock-soil slope; geogrid-box method; layered geogrid method, laboratory model; numerical model

1. Introduction

Soil stabilization using synthetic materials is a construction technique through which soil is reinforced using synthetic materials such as geotextile, geofabric, geogrid, geonet, and geomembrane. Depending on the soil type and the required performance, the applied geosynthetic would be different (Touze-Foltz *et al.* 2016). Among geosynthetics, geogrids have been used effectively to reinforce the soil structures such as embankments, roads, slopes, retaining walls and foundations. Geogrid is formed by a regular network of integrally connected tensile elements with openings of sufficient size to allow interlocking with surrounding soil, stone, or other geotechnical materials. Through the interlocking, the particles are confined and restrained from lateral movement (Liu *et al.* 2016).

During the last decade, the subject of foundation reinforcement using geogrids to improve load bearing capacity has attracted a great deal of attention and there have been wealth of research works on this fascinating subject (Binquet and Lee 1975, Shin and Das 1998, Kumar and Saran 2003, Dey 2010, Fahimifar *et al.* 2014). These studies have demonstrated that using geogrids improves the ultimate bearing capacity and decreases the settlement values to accepted limits. In many situations such as power pole footings and bridge abutments on sloping embankments, due to the space limits and non-availability of suitable construction sites, footings are built on/or adjacent to the slope. These footings have a lower bearing capacity and factor of safety compared to ones constructed on the flat ground. Hence, one of the essential objectives pursued by geotechnical engineers is to develop slope stability techniques to improve the bearing capacity of footings placed on the slope. Typical examples include modifying the slope surface geometry, chemical grouting, installing continuous or discrete retaining structures such as walls or piles, wire mesh installation and inclusion of geosynthetic reinforcement (Yoo 2001, Fattah *et al.* 2012).

Studies conducted on enhancing the bearing capacity of

∗Corresponding author, Assistant Professor
E-mail: pa.soltani@cc.iut.ac.ir
[a]Associate Professor
E-mail: gmoradi@tabrizu.ac.ir
[b]Ph.D. Candidate
E-mail: a.abdolmaleki@tabrizu.ac.ir
[c]M.Sc.
E-mail: tarhejame.geo@yahoo.com

ISSN: 2005-307X (Print), 2092-6219 (Online)

different types of footings can be generally divided into three main categories:

1. Studies conducted on reinforced slopes to develop limit equilibrium methods (Janbu 1954, Bishop 1955, Zhao 1996, Zornberg *et al.* 1998, Alkasawneh, *et al.* 2008, Dong-ping *et al.* 2016, Li *et al.* 2016);

2. Studies conducted on the bearing capacity behavior of footings placed on grounds reinforced with geosynthetics (Huang and Tatsuoka 1990, Omar *et al.* 1993, Das *et al.* 1994, Zhang *et al.* 2016, Hou *et al.* 2017) and

3. Studies conducted on the bearing capacity behavior of footings placed on slopes reinforced with geosynthetics (Selvadurai and Gnanendran 1989, El Sawwaf 2007, Alamshahi and Hataf 2009, Demir *et al.* 2014, Keskin and Laman 2014, Keskin and Laman 2014, Turker *et al.* 2014).

The studies performed on group 3 are scarce compared to those of groups 1 and 2. One of the possible measures to improve the bearing capacity of footings constructed on slopes is to reinforce the slope with layers of geogrid. This is achieved by the inclusion of multiple layers of geogrid at different depths and widths under the footing. In this regard, Keskin and Laman (2014) investigated the ultimate bearing capacity of strip footings rested on geogrid-reinforced sand slopes and reported the significant positive effect of stabilization on bearing capacity of these footings. Yoo (2001) performed a laboratory study to evaluate the bearing capacity behavior of footings constructed on sand slopes reinforced with geogrid. It was found that using geogrids considerably enhances the bearing capacity of strip footings on sloping ground and the magnitude of this improvement is a function of geogrid distribution. El Sawwaf (2007) evaluated the settlement reduction and bearing capacity behavior of strip footings built on soft clay slopes. To enhance the bearing capacity of the slope, the upper part of the slope replaced with geogrid-reinforced sand. The results demonstrated that using this method not only enhances the performance of the slope, but also leads to great reduction in the depth of reinforced sand layer required to achieve the allowable settlement. Demir *et al.* (2014) conducted a laboratory and numerical study to assess the bearing capacity of circular footing on geogrid-reinforced compacted granular fill layer overlying on natural clay deposit. It was shown that the degree of improvement depends on thickness of granular fill layer and properties and configuration of geogrid layers. Alamshahi and Hataf (2009) investigated the bearing capacity of strip footings on sand slopes reinforced with geogrid and grid-anchor. It was shown that the effect of the ordinary geogrid in improving the soil bearing capacity was less than that of the grid-anchor.

As stated earlier, the studies conducted on bearing capacity behavior of footings rested on sloping ground are more scarce compared to two other mentioned groups. Besides, the studies carried out in this field are mainly limited to the stabilization of soil slopes, especially those made of sand, while the studies that encompass the scope of investigating the bearing capacity behavior of rock-soil slopes scarcely exist. In a recent study, the authors (Fahimifar *et al.* 2014) introduced the geogrid-box method (GBM) as a new approach for reinforcement of rock slopes. In this method, the geogrid-boxes are filled up with crushed rocks in a way that a confined integrated system composed of rock materials and geogrid is obtained. In this study, the authors extend the application of this method for reinforcement of rock-soil slopes and investigate whether this new approach can be a satisfactory alternative for commonly practiced layered geogrid method (LGM).

To achieve the objectives of this study, a series of laboratory model tests were performed to study the bearing capacity behavior and settlement behavior of circular footings constructed on rock-soil slopes. To this end, a laboratory setup was designed and the slopes without reinforcement, reinforced with LGM, and reinforced with GBM were investigated. Numerical analyses were also performed using ABAQUS software and the results were compared with those of laboratory model tests.

2. Equipment and materials

2.1 Rock-soil materials

The rock-soil model used in this research is a 0-3″ mix of materials extracted from Kordan River (Karaj, Iran). The grain size distribution was determined using the dry sieving method and the results are shown in Fig. 1. According to AASHTO - T180-D the minimum and maximum unit weight of rock materials was found to be 1.97 and 2.11 g/cm^3, respectively. The moisture-density relation curve is presented in Fig. 2. A series of direct shear tests were performed to assess the shear strength properties of rock-soil materials. The values of internal friction angle (ϕ) and cohesion (c) were obtained as 49° and 0.06 kN/m^2, respectively. The results of direct shear test are presented in Fig. 3.

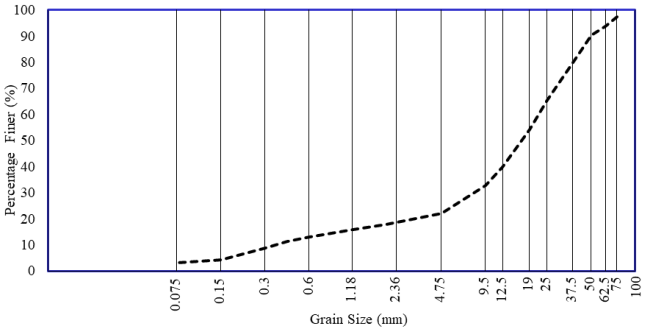

Fig. 1 Grain size distribution of rock-soil materials

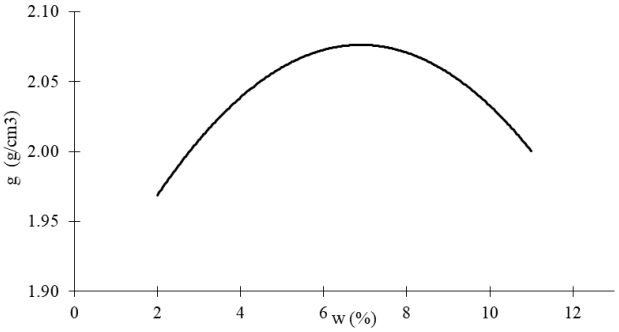

Fig. 2 Moisture-density relations curve of rock-soil materials

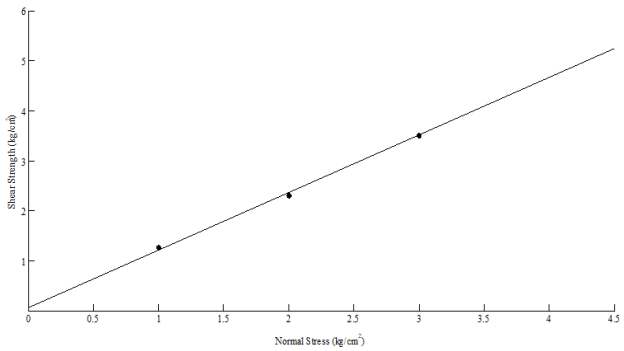

Fig. 3 Direct shear test curve of rock-soil materials

Table 1 Properties of materials used in the laboratory model and numerical analysis

Parameters	Unit	Value
Unit weight of rock-soil materials (γ)	g/cm^3	1.97
Modulus of elasticity (E)	kN/m^2	1.5×10^5
Internal friction angle (ϕ)	deg	49
Cohesion (c)	kN/m^2	0.06
Friction angle efficiency (E_φ)	%	103
Cohesion efficiency (E_c)	%	83
Poisson's ratio (ν)	--	0.27

Table 2 The engineering properties of geogrids

Parameters	Unit	Value
Polymer	-	PVC Coated Polyester
Mass per unit area	g/m^2	220
Aperture size	mm	25 × 25
UV resistance	%	> 93
Elongation at maximum load	%	14.6
Tensile Strength	N	2675
Flexural Rigidity	$mg.cm$	500000

To evaluate the effects of the confined box, the friction angle of rock-soil materials and geogrid (δ) and the adhesion of geogrid to rock-soil materials (c_a) were estimated according to ASTM-D5321. Using the obtained data, the friction angle efficiency (E_φ) and cohesion efficiency (E_c) were then calculated. The results obtained through these tests are summarized in Table 1.

2.2 Geogrid reinforcement

A commercially interwoven geogrid made of high modulus multifilament PET yarns was used as reinforcement element. Exterior of PET geogrid is coated with additional protective layer of PVC for UV resistance. The tensile strength of geogrid was determined in accordance to ASTM D6637-01, using Zwick tensile tester (model 1446, Germany).

Flexural rigidity of samples was determined in accordance to ASTM D1388. Typical physical and mechanical properties of geogrids are presented in Table 2.

3. Physical model

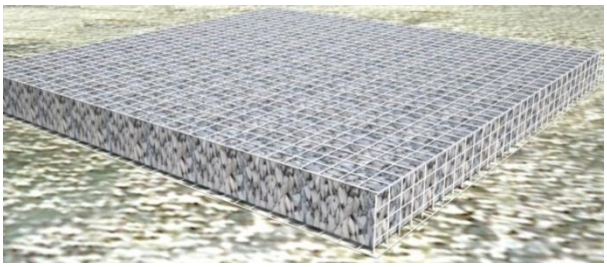

(a) Geogrid-box

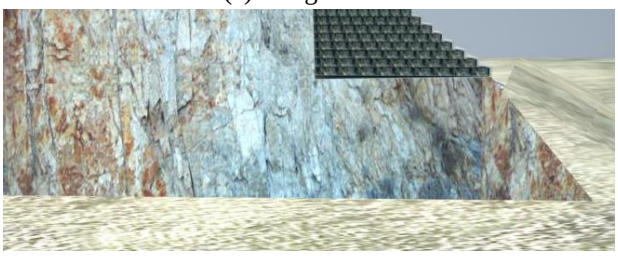

(b) Installation

Fig. 4 Schematic illustration of the GBM

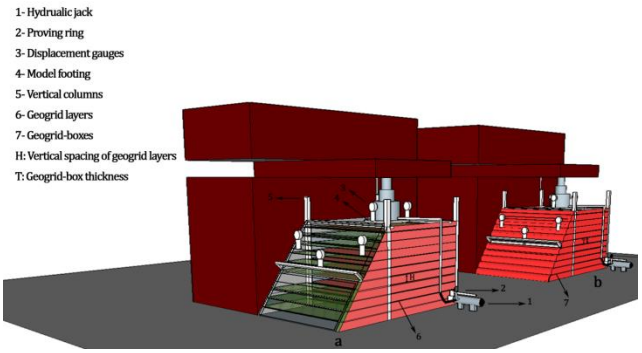

Fig. 5 Schematic view of test configuration (a) LGM (b) GBM

The main objective of this study is to evaluate the effect of GBM on the bearing capacity and failure mechanism of rock-soil slopes and comparing the obtained results with those of the traditional LGM. The GBM which was proposed by the authors (Fahimifar, Abdolmaleki *et al.* 2014) for reinforcement of rock slopes, is a stabilization technique through which the geogrid-boxes are filled up with rock-soil materials in a way that a confined integrated system composed of rock-soil materials and geogrid is obtained (Fig. 4(a)). The final prepared slope would be a set of reinforced boxes which are stacked on each other (Fig. 4(b)). This is different from the commonly practiced stabilization method, in which layers of geogrid are placed between rock-soil materials.

The physical test model was designed in a way that comparison of the load-settlement behavior of the slope reinforced with the GBM with that of one reinforced with LGM can be made. A series of laboratory model tests were performed in a test tank made of a steel frame. Model rock-soil slopes were constructed 990 mm in height and 1000 mm×1000 mm in plan with a slope angle of 60°. The dimensions were chosen based on the literature studies and the results of the finite element analysis (FEA) conducted prior to the model tests. To maintain plane strain conditions and prevent out-of-plane displacements, the slope model

was confined with four vertical columns and two horizontal profiles. Moreover, to observe the displacements occurred during the test and failure mode, one sidewall of the physical model was constructed using a 10 mm thick transparent Plexiglas. The inside walls of the test tank were polished smooth to minimize friction with the rock-soil materials as much as possible by using galvanized coat in the inside walls. In order to minimize the possible friction between the Plexiglas wall and the artificially made ground, transparency films were attached onto the inside walls. A schematic view of test configuration is illustrated in Fig. 5.

The proposed testing geometry of the slope was first marked on the transparent wall for reference. In all model tests, the average unit weight was kept constant at 1.97 g/cm^3 (loose-packing). This unit weight was achieved in the test tank using a carefully controlled raining technique. Rock-soil materials were pluviated using a constant deposition height in layers of 5 cm thick through a raining device that is moved to and fro to spread the materials uniformly. The consistency of the unit weight during raining was evaluated using small containers placed at various locations in the test tank. The height of raining to achieve the target unit weight was determined a priori by performing a series of trials with different heights of falls. In the LGM, the rock-soil materials were deposited in layers up to a desired height. On reaching the reinforcement level, a geogrid layer was placed and a layer of rock-soil materials was rained and so on. The rock-soil materials pouring process continued until the pointed height of the slope was reached. Great care was given to level the slope face using special rulers so that the relative density of the top surface was not affected. After preparing the slope at a predetermined location in the test tank the top surface was properly leveled. The same procedure was followed for the preparation of slopes reinforced with GBM with the exception that rock-soil materials were poured in geogrid-boxes of desired thickness.

4. Model testing

First, in order to obtain the better understanding of the A monotonic load was applied on the slope through an integrated system of hydraulic jack, high-pressure water hose, force gauge, manual pump, load weight, and circular loading plate. To measure occurred displacements, six 0.01 mm accuracy displacement gauges, six connection rods for gauge installation, and six magnet bases were installed. Before the test, using numerical analysis the critical points in terms of strain variations were detected and the displacement gauges were installed at these points. Consequently, displacement gauges 1, 2, and 3 were installed at 120° angle to each other on the circular loading plate, while displacement gauges 4, 5, and 6 were installed on the slope face. To increase the accuracy of the calculations, the displacement gauges were calibrated before each loading cycle. A schematic view of load application setup and the position of displacement gauges in the physical model are displayed in Fig. 5.

Loading tests were carried out using a circular footing made of steel with diameter and thickness of 300 and 30 mm, respectively. Vertical compressive loading was applied incrementally by a motor-controlled hydraulic jack having a loading rate of 0.5 mm/min at corresponding stress stages of 50 kPa. The loading rate was measured using a calibrated load cell. In each step, the settlements created in the footing at the critical parts of the slope were measured using displacement gauges in 1, 2, 4, and 8 minutes after the loading. The loading increment continued until either the applied vertical load clearly reduced or with a relatively slight increase in vertical load, a considerable settlement of footing is detected. Several tests were repeated at least twice to verify the repeatability and the consistency of the test data. The difference was considered to be small and neglected.

Table 3 The investigated designs

Design	Variable parameter	Design	Variable parameter
I	Unreinforced slope	VI	Box thickness: 25 cm
II	Box thickness: 15 cm	VII	Vertical spacing: 25 cm
III	Vertical spacing: 15 cm	VIII	Box thickness: 30 cm
IV	Box thickness: 20 cm	IX	Vertical spacing: 30 cm
V	Vertical spacing: 20 cm		

In this study, nine designs were considered and experimental tests were conducted to investigate the effect of GBM on the bearing capacity and failure mechanism of rock-soil slopes and compare the results with those of LGM. Table 3 summarizes all test programs. The primary purpose of design I was to evaluate the bearing capacity behavior of unreinforced rock-soil slope. Designs II, IV, VI, and VIII were planned to examine the effect of geogrid-box thickness and designs III, V, VII, and IX aimed to evaluate the effect of vertical spacing of geogrid layers on the bearing capacity and settlement behavior of circular footing. Finally, the bearing capacity behavior and failure mechanism of the designs were investigated in four groups including (designs I, II, and III), (designs I, IV, and V), (designs I, VI, and VII), and (designs I, VIII, and IX).

5. Numerical modeling

A series of 3D finite element analysis (FEA) were performed on a footing-slope system using ABAQUS software, in order to verify the laboratory model tests and perceive internal deformation of reinforced and unreinforced rock-soil materials. The merits of developing such a finite element model are that it can be used to model various conditions which have not been examined experimentally. The geometry of the model footing-slope system was assumed to be the same as the laboratory model. The angle of slope, the material of steel plate for footing, geogrid and rock-soil, and loading plate dimensions were the same as those assigned in laboratory tests.

To model rock-soil material the solid element was used while to describe the elasto-plastic behavior of materials the Mohr-coulomb model was employed. In order to model the circular loading plate, the solid element with elastic behavior and steel characteristics was applied. Furthermore, to model the geogrids, the Shell elements were used. To

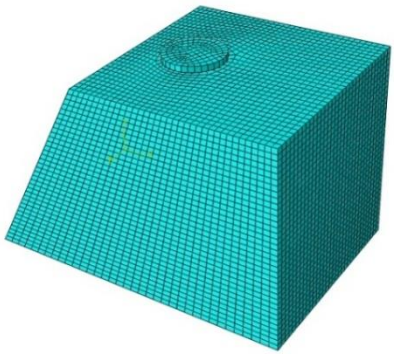

(a) Generated mesh

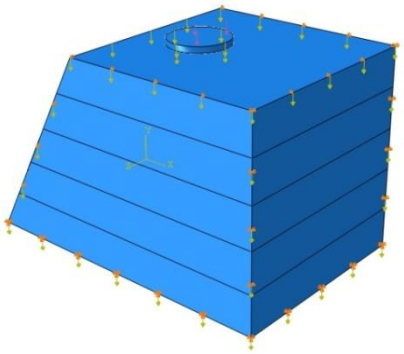

(b) Boundary conditions

Fig. 6 The slope model

present behavior of the geogrids, the plastic behavior model with a pure tension was applied. The interaction between the geogrid and rock-soil materials was modeled at both sides by means of interface elements. Hexagonal and quad elements were used for Solid and Shell elements, respectively.

The analyzed prototype slope geometry, generated mesh and boundary conditions are presented in Fig. 6.

6. Results and discussions

In order to evaluate the settlement behavior of rock-soil slope loaded under a circular footing, the average settlement recorded from displacement gauges 1, 2, and 3 installed on the loading plates were measured in each loading stage (U). The footing settlement was non-dimensionalized by footing diameter (B) and expressed in the form of (U/B). In this section, the relation of vertical loading pressure (q) to settlement ratio (U/B) for various designs is presented and discussed.

When dense-packing materials are subjected to vertical pressure loading, the ultimate bearing capacity (q_u) would be distinctly observed in the peak of load-settlement curve. This behavior was not observed in any of the reinforced laboratory test models and numerical analysis. This is attributed to the loose-packing nature of rock-soil materials. Therefore, the increase in loading is accompanied with aggregates settlement, leading to no peak in the load-settlement curve. In these cases choosing a single value of ultimate bearing capacity may be highly subjective. Hence, to make the results comparable, the ultimate bearing capacity was taken as the point at which the settlement reaches 10% of the footing diameter.

A noticeable uplift on the slope also implies failure initiation. To measure uplift, the displacement values recorded by displacement gauges installed on the slope face were recorded at each loading stage.

To assess the effects of GBM on the bearing capacity behavior of rock-soil slopes and compare the results with those of traditional LGM and unreinforced slope, the dimensionless parameters BCR_1, BCR_2, BCR_3, BCR'_1, BCR'_2, and BCR'_3 were defined according to the following equations

$$BCR_1 = \frac{q_{URB}}{q_{UR}} \qquad BCR'_1 = \frac{q'_{URB}}{q'_{UR}}$$
$$BCR_2 = \frac{q_{URB}}{q_U} \qquad BCR'_2 = \frac{q'_{URB}}{q_U} \tag{1}$$
$$BCR_3 = \frac{q_{UR}}{q_U} \qquad BCR'_3 = \frac{q'_{UR}}{q'_U}$$

where BCR_1, BCR_2, and BCR_3 are the bearing capacity ratios obtained using laboratory model tests and BCR'_1, BCR'_2, and BCR'_3 are the bearing capacity ratios obtained through the numerical analysis. q_{URB} and q'_{URB} denote the ultimate bearing capacity of the slopes reinforced with GBM in the laboratory and numerical models, respectively; q_{UR} and q'_{UR} are the ultimate bearing capacity of the slopes reinforced with LGM in the laboratory and numerical models, respectively; and q_U and q'_U are the ultimate bearing capacity of unreinforced slopes in the laboratory and numerical models, respectively. According to the above definition:

- The BCR_1 values indicate monotonic bearing capacity improvement of GBM-reinforced slope in relation to the LGM-reinforced slope.
- The BCR_2 values indicate monotonic bearing capacity improvement of GBM-reinforced slope in relation to the unreinforced slope.
- The BCR_3 values indicate monotonic bearing capacity improvement of LGM-reinforced slope in relation to the unreinforced slope.

6.1 Group A: Comparing designs I, II, and III

As depicted in Fig. 7, the slope failure in design I (unreinforced slope) instantly occurs during the first stage of loading, while the slope reinforced with GBM experiences some cracking under the effect of ultimate load. This is ascribed to the mobilized passive earth resistance of aggregates confined in the geogrid-box along with effective interlocking of aggregates and geogrid apertures, which restrict the spreading of slope and lateral deformations of rock-soil materials.

Fig. 8 illustrates typical variations of bearing capacity pressures (q) with settlement ratios (U/B) for the laboratory and numerical modeling of designs II and III. As can be observed, in comparison with LGM, the GBM improves both the initial stiffness (initial slope of the $q - U/B$ curves) and the bearing load at the same settlement level.

The measured ultimate bearing load of circular footing resting on reinforced slope with geogrid-box with thickness of 15 cm (design II) is $q_{URB} = 248.63\ kPa$. This means

Fig. 7 The unreinforced slope failure

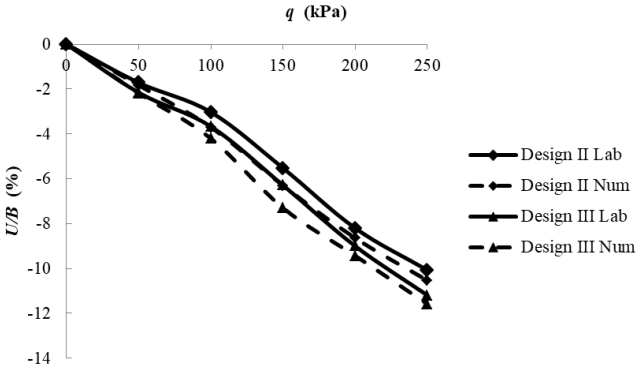

Fig. 8 Variations of U/B with q for designs II and III

that when the stress is $248.63\ kPa$, the average settlement recorded by gauges 1, 2, and 3 exceeds 10% of the loading plate diameter. For design III, the physical model gives an output of $q_{UR} = 222.78\ kPa$, implying that when the slope is reinforced with geogrid layers with vertical spacing of 15 cm, the average settlement recorded by the gauges exceeds 10% of the loading plate diameter at the stress of 222.78 kPa. The corresponding theoretical ultimate bearing loads obtained from the FEA are $q'_{URB} = 236.02$ and $q'_{UR} = 214.22\ kPa$. Based on the outputs of laboratory and numerical tests, the bearing capacity ratios for this group are as follows

$$\begin{aligned} BCR_1 &= 1.116 & BCR'_1 &= 1.101 \\ BCR_2 &= 24.863 & BCR'_2 &= 23.602 \\ BCR_3 &= 22.278 & BCR'_3 &= 21.422 \end{aligned} \quad (2)$$

The calculated value of BCR_1 indicates that when the vertical spacing of layers and thickness of boxes are $15\ cm$, the ultimate bearing capacity of reinforced slope with GBM 11.16% is higher than that of reinforced slope with LGM. This is due to the fact that the confined rock-soil materials between the geogrid act as a reinforced rock-soil beam with enhanced shear strength, and thus transfers the major part of the footing load deeper into the adjacent stable layers of soils leading to a wider and deeper failure zone. The BCR_2 values show a 24.8 times increase in bearing capacity of the slope reinforced with GBM compared to the unreinforced slope. Additionally, the BCR_3 values indicate a 22.2 times increase in bearing capacity of the slope reinforced with LGM compared to the unreinforced slope. These results are discussed in the following sections.

The results also reveal that the average settlement in GBM is lower compared to the LGM. This is attributed to the stress distribution in a wider and deeper area in GBM that causes a larger mass of rock-soil materials resist the applied load. This restricts the spreading of slope and lateral deformation of rock-soil materials.

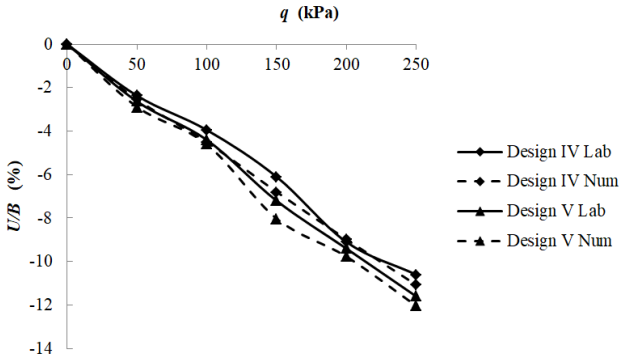

Fig. 9 Variations of U/B with q for designs IV and V

Uplift is also one of the indicators of slope failure. In design II, the uplift values recorded by gauges 4, 5, and 6 at stress of 250 kPa are 1.2, 1.4, and 0.56 mm in, respectively. As previously discussed, higher values of uplift recorded by gauges 4 and 5 are due to the proximity of these gauges to the lateral solid walls of slope model and their greater distance from the center of the slope face. Since the distance from the lateral solid walls affects the uplift values, the effect of this parameter must be evaluated. Thus, the test was repeated by adjusting the distance of gauges 4 and 5 from lateral walls from 25 to 35 cm. The uplift values recorded in this state indicate a considerable decrease, as it was lowered to 0.6 and 0.64 mm in gauges 4 and 5, respectively. These results imply the acceptable accuracy of gauge 6 in assessing the uplift induced by the vertical loading pressure. Based on the outputs of laboratory and numerical modelings, the uplift values in GBM are less than that of LGM. In design III at the stress of 250 kPa, the uplift recorded in gauge 6 is 0.71 mm implying the larger displacement of materials in LGM compared to GBM.

The results show that although the bearing capacities obtained from the FEA are smaller than those of physical models, there is an acceptable agreement between the outputs of laboratory and numerical modelings. The observed discrepancy may be attributed to the model and rock-soil materials parameters chosen and the differences of the boundary conditions in numerical and experimental models.

6.2 Group B: Comparing designs I, IV, and V

Fig. 9 illustrates typical variations of the bearing capacity pressures with settlement ratios for the laboratory and numerical modeling of designs IV and V. For designs IV and V, the measured bearing loads are $q_{URB} = 227.38$ and $q_{UR} = 212.27\ kPa$, respectively. Based on the outputs of laboratory and numerical tests, the bearing capacity ratios for this group are as follows

$$\begin{aligned} BCR_1 &= 1.071 & BCR'_1 &= 1.067 \\ BCR_2 &= 22.738 & BCR'_2 &= 21.966 \\ BCR_3 &= 21.227 & BCR'_3 &= 20.588 \end{aligned} \quad (3)$$

As is observed, replacing LGM with GBM leads to a 7.1% increase in the BCR_1 value. Also, BCR_2 value indicates a 22.7 times increase in the bearing capacity of the slope reinforced with GBM compared to the that of unreinforced slope.

The uplift values in gauge 6 at the stress of 250 kPa in designs IV and V are 0.863 and 1.503 mm, respectively that suggest a 43% decrease in uplift value at this stress level.

6.3 Group C: Comparing designs I, VI, and VII

The load-settlement curves for laboratory and numerical modelings in designs VI and VII are shown in Fig. 10. For designs VI and VII, the outputs of laboratory modelings are $q_{URB} = 197.91\ kPa$ and $q_{UR} = 188.82\ kPa$, respectively. Based on the outputs of laboratory and numerical modellings, the bearing capacity values for this group are as follows

$$\begin{aligned} BCR_1 &= 1.048 & BCR'_1 &= 1.044 \\ BCR_2 &= 19.791 & BCR'_2 &= 19.635 \\ BCR_3 &= 18.882 & BCR'_3 &= 19.147 \end{aligned} \quad (4)$$

BCR_1 value indicates a 4.8% increase in bearing capacity by replacing the LGM with GBM. Moreover, BCR_2 shows a 19.8 times increase in the bearing capacity of the slope reinforced with GBM compared to the that of the unreinforced slope.

The uplift recorded in gauge 6 in design VI and design VII at the stress of 200 kPa are 0.6 and 2.3 mm, respectively, indicating a 74% decrease in uplift at this stress level.

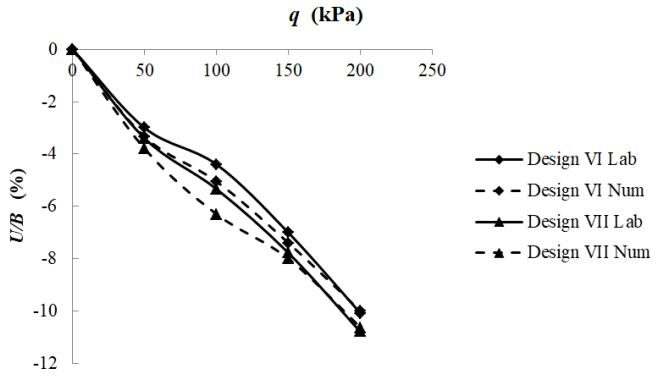

Fig. 10 Variations of U/B with q for designs VI and VII

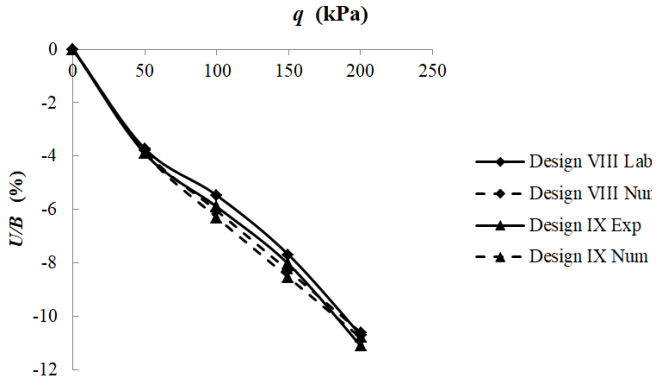

Fig. 11 Variations of U/B with q for designs VIII and IX

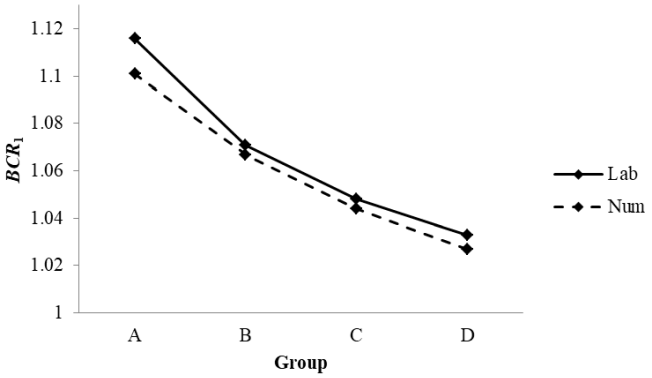

Fig. 12 Variations of BCR_1 in groups *A* through *D*

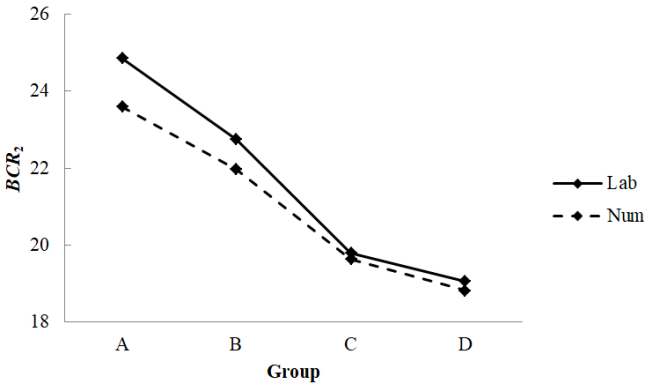

Fig. 13 Variations of BCR_2 in groups *A* through *D*

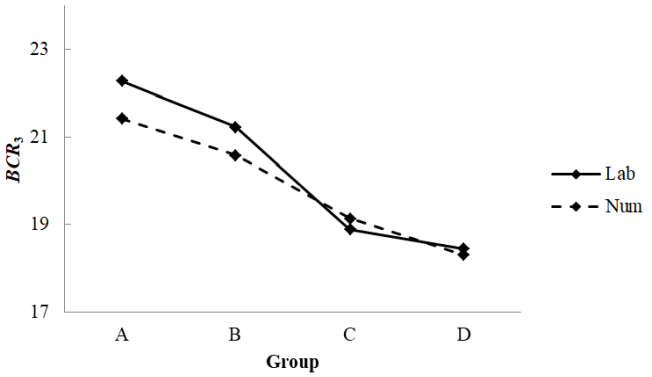

Fig. 14 Variations of BCR_3 in groups *A* through *D*

6.4 Group D: Comparing designs I, VIII, and IX

The load-settlement curves of laboratory and numerical models for designs VIII and IX are presented in Fig. 11. In designs VIII and IX, the outputs of laboratory modelings are $q_{URB} = 190.59\ kPa$ and $q_{UR} = 184.51\ kPa$, respectively. Based on the outputs of laboratory and numerical modelings, the bearing capacity ratios of this group are as follows

$$\begin{aligned} BCR_1 &= 1.033 & BCR'_1 &= 1.027 \\ BCR_2 &= 19.059 & BCR'_2 &= 18.816 \\ BCR_3 &= 18.451 & BCR'_3 &= 18.310 \end{aligned} \quad (5)$$

In this case, the BCR_1 value indicates a 3.3% increase in the bearing capacity by replacing the LGM with GBM. In addition, BCR_2 shows a 19 times increase in the bearing

capacity of the slope reinforced with GBM compared to the bearing capacity of the slope without reinforcement.
The uplift recorded in gauge 6 in designs VIII and IX at 200 kPa are 0.68 and 2.43 mm, implying a 72% decrease in uplift at this stress level.

Figs. 12-14 provide a comparison of BCR_1, BCR_2, and BCR_3 values in laboratory and numerical modelings for groups A, B, C and D. Fig. 12 shows monotonic bearing capacity improvement of reinforced slope with GBM in relation to the slope reinforced with LGM for groups A to D. As can be seen, the rate of load improvement becomes much less by increasing the distance of reinforcements, as shown by BCR_1 approaching unity. As is observed, although the BCR_1 values obtained from the numerical analysis seems to be smaller than those of the laboratory model tests, the common trends of the manner in which BCR_1 differs with the distance of reinforcement are in good agreement with those from the laboratory model tests. Fig. 13 shows that by increasing the thickness of box from 15 to 25 cm, a sharp decrease in BCR_2 values is observed, beyond which no considerable drop is noticed. The same trend is observed for the slopes reinforced with LGM. Again the finite element results are close to those of laboratory model tests and agree with the same trends.

Comparison of the designs in groups A to D reveals that by increasing the vertical spacing of geogrid layers and thickness of geogrid-boxes, the bearing capacity of slope decreases. The results of numerical analysis establish that increase in the distance between the stabilizations leads to a declination in stress distribution and displacement contours and as a result, a decrease in bearing capacity. However, the rate of decrease in the distribution of displacement contours and loading-induced stresses in GBM is less than that of LGM. These results are described further in the following section. The results also indicate that for the same footing load, the settlement ratio increases with increasing the vertical spacing of geogrid layers and thickness of geogrid-box.

7. Failure mechanism

In this section, the failure mechanisms of the circular footing rested on a footing-slope system is investigated using the 3D finite element analysis. Figs. 15-17 illustrate the failure mechanisms on the basis of displacements contours in the numerical analysis for designs I, II and III. Note that same plots were obtained for designs IV to IX, but not presented for the sake of brevity. The displacement contours of a loaded circular footing resting on an unreinforced rock-soil slope are shown in Fig. 15. As is observed, the displacement contours are concentrated underneath the footing and are very shallow. Thus, a smaller area of rock-soil materials resists the applied load and consequently, the bearing capacity of the slope is small. As can be observed in Figs. 16 and 17, for the reinforced slopes especially the slopes reinforced with GBM, the displacement contours are broadly distributed in the rock-soil mass beneath the footing in greater width and depth than that in the unreinforced slope. The mobilized tension in the reinforcement not only allows the geogrid to resist the imposed horizontal shear stresses built up in the rock-soil

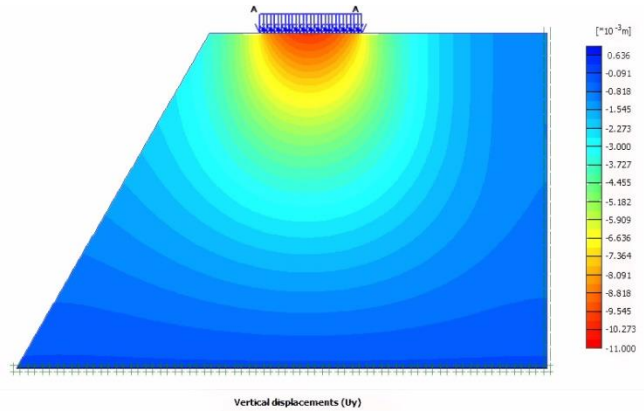

Fig. 15 Displacement contours of unreinforced rock-soil slope

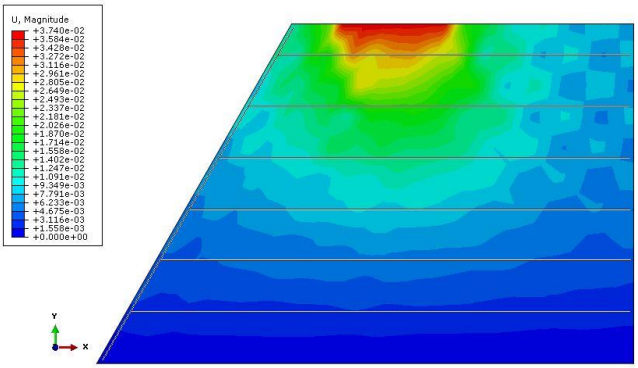

Fig. 16 Displacement contours in the rock-soil slope for design II

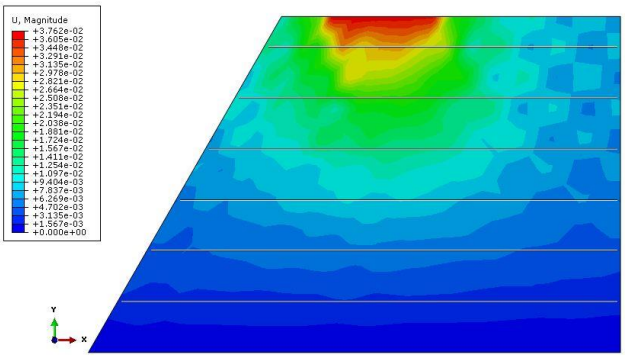

Fig. 17 Displacement contours in the rock-soil slope for design III

mass underneath the footing, but also spreads them deeper into the adjacent stable layers of soils and leads to a wider and deeper failure zone.

The results of numerical analysis showed that, the smaller the vertical spacing of geogrid layers is, the wider the distribution of displacement contours and greater their depth would be. As a result, a larger distribution of loading-induced stresses and longer failure surface would be developed and hence greater bearing capacity is achieved. By decreasing the geogrid-box thickness, the expansion trend of the failure surface is more remarkable when compared with that for the reinforced slope with LGM. By reducing the thickness of geogrid-boxes, the distribution and depth of displacement contours increases and a larger

failure zone is developed. A larger failure zone, which in turn means a longer failure surface, would render a higher bearing capacity.

8. The scale effect and limitations

Laboratory modeling is among the most important approaches for dealing with limitations and evaluating the results of analytical and numerical methods. This approach is very common in civil engineering for validating the numerical and analytical models. In general, laboratory modeling can be carried out through either a large-scale model or a small-scale model. Large-scale modeling is generally performed with the real site conditions, such as the ground conditions, loads and stress levels. Hence, the results obtained from this type of modeling are more accurate than those of small-scale modeling. However, large-scale modeling is not always possible due to its operational and financial limitations. Small-scale laboratory model tests are easier to operate due to their small sizes and the cost is considerably less than large-scale in-situ tests. Therefore the small-scale tests are carried out widely as an alternative for large-scale models (Yoo 2001, El Sawwaf 2007, Alamshahi and Hataf 2009, Azzam and Nasr 2014, Keskin and Laman 2014). It has been well-established that due to the scale effects and the nature of fine-grained soils, soils may not play the same role in the laboratory models as in the prototype and involve a high scale-error (El Sawwaf 2007, Keskin and Laman 2014). However, the small-scale laboratory tests on coarse-grained rock-soil materials, unlike the fine-grained soils, do not involve high errors (Vesic 1974, Hirofumi *et al.* 2003, Jaeger *et al.* 2009). Moreover, in this work, the model tests were performed on a small-scale model footing, while the used geogrids had the same physical and mechanical properties and dimensions as in the prototype. Therefore, due to the scale effects and use of prototype geogrid, the results of laboratory models may be affected, both in qualitative and quantitative aspects. It was illustrated in previous sections that the main objectives of this study are to compare the GBM and LGM and investigate the failure mechanism in reinforced rock-soil slopes. Since in all experimental models same geogrids were used, this limitation is not highly noted. Nevertheless, further studies are required to ascertain the validity of the findings in this study using large-scale model tests. In order to conduct large-scale analysis, it is necessary to evaluate the performance and accuracy of numerical simulations. To this end, in this study small-scale laboratory-tests were conducted to verify numerical models in term of material models, boundary conditions, etc. High consistency was observed between the numerical and laboratory results.

Furthermore, this study has not investigated the effects of changes of some variables such as model dimensions, slope angle, location of footing relative to the slope, tensile stiffness and strength of reinforcements on the bearing capacity of rock-soil slopes reinforced with GBM. The effects of these parameters are currently being investigated by the authors, the results of which are due to be reported. The present work can provide a proper base ground for further works in this area and its results can be compared with those of large-scale and centrifugal modeling tests.

9. Conclusions

In this study, the novel geogrid-box method (GBM) was introduced for reinforcing rock-soil slopes. The effect of this method on the bearing capacity and failure mechanism of slopes was investigated by conducting a series of laboratory model tests and finite element analysis. The results were then compared with those of commonly practiced layered geogrid method (LGM). On the basis of the results of the laboratory model tests and finite element analyses, the main outlines of this work are as follows:

1. Reinforcement of rock-soil slopes using LGM and GBM significantly increases the bearing capacity of slope. The degree of increase depends on the vertical spacing of geogrid layers and box thickness. More beneficial effect of the reinforcement can be driven for the smaller vertical spacing and box thickness.
2. Based on the studied designs, the ultimate bearing capacity of the slope reinforced with GBM can be 11.16% higher than that of the slope reinforced with LGM.
3. The BCR_2 values obtained through the investigated designs represent a 24.8 times increase in the ultimate bearing capacity of the rock-soil slope reinforced with GBM compared to the unreinforced slope.
4. The BCR_3 values obtained through the investigated designs imply a 22.3 times increase in the ultimate bearing capacity of the rock-soil slope reinforced with LGM compared to the unreinforced slope.
5. In the unreinforced rock-soil slope, the area under loading-induced stress is smaller compared to the reinforced slopes and a high level of stress concentration is observed in the regions located near the circular footing.
6. The results clearly show that the effect of the commonly practiced LGM in improving the bearing capacity of rock-soil slopes is less than that of the GBM.
7. For the reinforced slopes especially the slopes reinforced with GBM, the displacement contours are widely distributed in the rock-soil mass underneath the footing in greater width and depth than that in the unreinforced slope. This is attributed to the stress distribution mode and stress transfer in the GBM.
8. The average settlement in the GBM compared to the LGM is lower due to the stress distribution in a broader and deeper area, which causes a larger mass of rock-soil materials resist the applied load.
9. The uplift level in the GBM is less than that of the LGM.
10. A good agreement was observed between the laboratory model tests and numerical results.

References

Alamshahi, S. and Hataf, N. (2009), "Bearing capacity of strip footings on sand slopes reinforced with geogrid and grid-anchor", *Geotext. Geomembr.*, **27**(3), 217-226.

Alkasawneh, W., Husein Malkawi, A.I., Nusairat, J.H. and

Albataineh, N. (2008), "A comparative study of various commercially available programs in slope stability analysis", *Comput. Geotech.*, **35**(3), 428-435.
Azzam, W.R. and Nasr, A.M. (2014), "Bearing capacity of shell strip footing on reinforced sand", *J. Adv. Res.*, **6**(5), 727-737.
Binquet, J. and Lee, K.L. (1975), "Bearing capacity tests on reinforced earth slabs", *J. Geotech. Eng. Div.*, **101**(12), 1241-1255.
Bishop, A.W. (1955), "The use of the slip circle in the stability analysis of slopes", *Geotechnique*, **5** 7-17.
Das, B.M., Shin, E.C. and Omar, M.T. (1994), "The bearing capacity of surface strip foundations on geogrid-reinforced sand and clay-a comparative study", *Geotech. Geol. Eng.*, **12**(1), 1-14.
Demir, A., Yildiz, A., Laman, M. and Ornek, M. (2014), "Experimental and numerical analyses of circular footing on geogrid-reinforced granular fill underlain by soft clay", *Acta Geotechnica*. **9**(4), 711-723.
Dey, A. (2010), "Bearing capacity of reinforced foundations: statistical approach and sensitivity analysis", *Proc. Soc. Behav. Sci.*, **2**(6), 7642-7643.
Dong-ping, D., Liang, L., Jian-feng, W. and Lian-heng, Z. (2016), "Limit equilibrium method for rock slope stability analysis by using the Generalized Hoek-Brown criterion", *J. Rock Mech. Min. Sci.*, (89), 176-184.
El Sawwaf, M.A. (2007), "Behavior of strip footing on geogrid-reinforced sand over a soft clay slope", *Geotext. Geomembr.*, **25**(1), 50-60.
Fahimifar, A., Abdolmaleki, A. and Soltani, P. (2014), "Stabilization of rock slopes using geogrid boxes", *Arab. J. Geosci.*, **7**(2), 609-621.
Fattah, M.Y., Al-Shakarchi, Y.J. and Al-Hadidi, M.T. (2012), "A procedure for analysing reinforced embankments", *Arab. J. Sci. Eng.*, **37**(6), 1547-1555.
Hirofumi, F., Jun'ichi, N. and Koichi, T. (2003), "A study on the scale effect of ultimate bearing capacity on rock fill", *Mon. Rep. Civ. Eng. Res. Inst.*, **600**, 21-28.
Hou, J., Zhang, M.X., Dai, Z.H., Li, J.Z. and Zeng, F.F. (2017), "Bearing capacity of strip foundations in horizontal-vertical reinforced soils", *Geotext. Geomembr.*, **45**(1), 29-34.
Huang, C.C. and Tatsuoka, F. (1990), "Bearing capacity of reinforced horizontal sandy ground", *Geotext. Geomembr.*, **9**(1), 51-82.
Jaeger, J.C., Cook, N.G.V. and Zimmerman, R. (2009), *Fundamentals of Rock Mechanics*, John Wiley & Sons, New York, U.S.A.
Janbu, N. (1954), "Applications of composite slip surfaces for stability analysis", *Proceedings of the European Conference on Stability of Earth Slope*, Stockholm, Sweden, September.
Keskin, M.S. and Laman, M. (2014), "Experimental and numerical studies of strip footings on geogrid-reinforced sand slope", *Arab. J. Sci. Eng.*, **39**(3), 1607-1619.
Keskin, M.S. and Laman, M. (2014), "Experimental study of bearing capacity of strip footing on sand slope reinforced with tire chips", *Geomech. Eng.*, **6**(3), 249-262.
Kumar, A. and Saran, S. (2003), "Bearing capacity of rectangular footing on reinforced soil", *Geotech. Geol. Eng.*, **21**(3), 201-224.
Li, D.Q., Xiao, T., Cao, Z.J., Phoon, K.K. and Zhou, C.B. (2016), "Efficient and consistent reliability analysis of soil slope stability using both limit equilibrium analysis and finite element analysis", *Appl. Math. Model.*, **40**(9-10), 5216-5229.
Liu, S., Huang, H., Qiu, T. and Kwon, J. (2016), "Effect of geogrid on railroad ballast particle movement", *Transport. Geotech.*, **9** 110-122.
Omar, M.T., Das, B.M., Puri, V.K. and Yen, S.C. (1993), "Ultimate bearing capacity of shallow foundations on sand with geogrid reinforcement", *Can. Geotech. J.*, **30**(3), 545-549.
Selvadurai, P.S. and Gnanendran, C.T. (1989), "An experimental study of a footing located on a sloped fill: Influence of a soil reinforcement layer", *Can. Geotech. J.*, **26**(3), 467-473.
Shin, E.C. and Das, B.M. (1998), "Ultimate bearing capacity of strip foundation on geogrid-reinforced clay slope", *KSCE J. Civ. Eng.*, **2**(4), 481-488.
Touze-Foltz, N., Bannour, H., Barral, C. and Stoltz, G. (2016), "A review of the performance of geosynthetics for environmental protection", *Geotext. Geomembr.*, **44**(5), 656-672.
Turker, E., Sadoglu, E., Cure, E. and Uzuner, B.A. (2014), "Bearing capacity of eccentrically loaded strip footings close to geotextile-reinforced sand slope", *Can. Geotech. J.*, **51**(8), 884-895.
Vesic, A.S. (1974), "Analysis of ultimate loads of shallow foundations", *J. Rock Mech. Min. Sci. Geomech. Abstr.*, **11**(11), A230.
Yoo, C. (2001), "Laboratory investigation of bearing capacity behavior of strip footing on geogrid-reinforced sand slope", *Geotext. Geomembr.*, **19**(5), 279-298.
Zhang, Y., Andersen, K.H. and Tedesco, G. (2016), "Ultimate bearing capacity of laterally loaded piles in clay-some practical considerations", *Mar. Struct.*, **50**, 260-275.
Zhao, A. (1996), "Limit analysis of geosynthetic-reinforced soil slopes", *Geosynth.*, **3**(6), 721-740.
Zornberg, J.G., Sitar, N. and Mitchell, J.K. (1998), "Limit equilibrium as basis for design of geosynthetic reinforced slopes", *J. Geotech. Geoenviron. Eng.*, **124**(8), 684-698.
Zornberg, J.G., Sitar, N. and Mitchell, J.K. (1998), "Performance of geosynthetic reinforced slopes at failure", *J. Geotech. Geoenviron. Eng.*, **124**(8), 670-683.

JS